Developmental Biology **214,** 23–37 (1999)
Article ID dbio.1999.9406, available online at http://www.idealibrary.com on IDEAL®

Restricted Expression of Cardiac Myosin Genes Reveals Regulated Aspects of Heart Tube Assembly in Zebrafish

Deborah Yelon, Sally A. Horne, and Didier Y. R. Stainier[1]

Department of Biochemistry and Biophysics and Programs in Human Genetics and Developmental Biology, University of California, San Francisco, San Francisco, California 94143-0448

The embryonic vertebrate heart is divided into two major chambers, an anterior ventricle and a posterior atrium. Although the fundamental differences between ventricular and atrial tissues are well documented, it is not known when and how cardiac anterior–posterior (A–P) patterning occurs. The expression patterns of two zebrafish cardiac myosin genes, *cardiac myosin light chain 2* (*cmlc2*) and *ventricular myosin heavy chain (vmhc*), allow us to distinguish two populations of myocardial precursors at an early stage, well before the heart tube forms. These myocardial subpopulations, which may represent the ventricular and atrial precursors, are organized in a medial–lateral pattern within the precardiac mesoderm. Our examinations of *cmlc2* and *vmhc* expression throughout the process of heart tube assembly indicate the important role of an intermediate structure, the cardiac cone, in the conversion of this early medial–lateral pattern into the A–P pattern of the heart tube. To gain insight into the genetic regulation of heart tube assembly and patterning, we examine *cmlc2* and *vmhc* expression in several zebrafish mutants. Analyses of mutations that cause cardia bifida demonstrate that the achievement of a proper cardiac A–P pattern does not depend upon cardiac fusion. On the other hand, cardiac fusion does not ensure the proper A–P orientation of the ventricle and atrium, as demonstrated by the *heart and soul* mutation, which blocks cardiac cone morphogenesis. Finally, the *pandora* mutation interferes with the establishment of the early medial–lateral myocardial pattern. Altogether, these data suggest new models for the mechanisms that regulate the formation of a patterned heart tube and provide an important framework for future analyses of zebrafish mutants with defects in this process.

Key Words: **ventricle; atrium; *heart and soul*; *casanova*; *pandora*; cardia bifida.**

INTRODUCTION

Organogenesis requires the proper orientation of a forming organ relative to established embryonic axes, but the mechanisms by which organ polarity is coordinated with embryonic polarity are poorly understood. In the case of the embryonic vertebrate heart, this coordination is critical, since the correct alignment of the cardiac anterior–posterior (A–P) axis with the embryonic A–P axis is essential for the establishment of proper blood flow. The embryonic vertebrate heart is a simple two-layered tube, composed of an outer myocardium and inner endocardium, that forms from the fusion of bilateral regions of precardiac mesoderm (for a review, see Fishman and Chien, 1997). Cardiac polarity is evident in the heart's simple A–P pattern: the heart tube is divided into two major chambers, an anterior ventricle and a posterior atrium. These two chambers are morphologically distinct; furthermore, the ventricular myocardium differs from the atrial myocardium by many physiological, histological, and molecular criteria, including characteristic rates of contractility (DeHaan, 1965; Satin *et al.*, 1988) and chamber-specific programs of gene expression (Franco *et al.*, 1998; Lyons, 1994). Although the fundamental distinction between ventricular and atrial myocardial cells is well documented in many vertebrates, it is not understood when and how cardiac A–P patterning occurs.

Fate mapping studies suggest that ventricular and atrial

[1] To whom correspondence should be addressed at Department of Biochemistry and Biophysics, University of California, San Francisco, 513 Parnassus Avenue, San Francisco, CA 94143-0448. Fax: (415) 476-3892. E-mail: didier_stainier@biochem.ucsf.edu.

0012-1606/99 $30.00

lineages may separate very early, even prior to gastrulation. For instance, labeling a single blastomere in a zebrafish midblastula embryo results in labeled progeny in either the ventricle or the atrium, but never in both chambers (Stainier *et al.*, 1993). Experiments in chick embryos have demonstrated that cells in rostral regions of the cardiogenic portion of the primitive streak later reside in the ventricle, while cells located more caudally within the streak contribute to the atrium (Garcia-Martinez and Schoenwolf, 1993). Shortly after the end of gastrulation, explants of anterior and posterior regions of chick precardiac mesoderm exhibit restricted developmental potential (Yutzey *et al.*, 1995). Together, these data are consistent with the existence of physically distinct ventricular and atrial fields within the blastula that do not intermingle during gastrulation or cardiac fusion. Nevertheless, these previous studies do not address a number of important issues, including when and how these cells become specified into ventricular and atrial precursors and when lineage-specific differentiation begins.

Overt chamber-specific differentiation has been detected *in vivo* only during or after the initiation of cardiac fusion. For instance, a few chamber-specific genes exhibit regionalized expression within the forming heart tube before the cardiac chambers are morphologically demarcated. Expression of a chick atrial myosin heavy chain gene (*AMHC1*) is restricted to the preatrial portion of the forming heart tube (Yutzey *et al.*, 1994). Similarly, expression of the murine ventricular myosin light chain gene *mlc2v* is restricted to preventricular regions during early phases of heart tube assembly (O'Brien *et al.*, 1993; Lyons *et al.*, 1995). Thus, chamber specification surely precedes chamber demarcation, but there is no clear molecular evidence of an early pattern within the physically separate bilateral regions of precardiac mesoderm.

Here, we report and utilize two zebrafish genes that distinguish myocardial subpopulations: while *cardiac myosin light chain 2* is expressed throughout the heart tube, *ventricular myosin heavy chain* is restricted to the ventricle. Interestingly, the expression patterns of these genes at early stages reveal two distinct subpopulations of myocardial precursors that are organized in a medial–lateral pattern; these subsets may represent ventricular and atrial precursors. Our examinations of *cmlc2* and *vmhc* expression throughout the process of heart tube assembly indicate the critical role of an intermediate structure, the cardiac cone, in the conversion of this early medial–lateral pattern into the A–P pattern of the heart tube. Additionally, the patterns of *cmlc2* and *vmhc* expression in several zebrafish mutants reveal genetic requirements for the assembly of a patterned heart tube. Specifically, the phenotypes of *casanova* and *heart and soul* mutants illuminate the relationship between cardiac A–P patterning and cardiac fusion. Furthermore, we show that *pandora* is essential for early steps of myocardial patterning. Based on these data, we propose new models for the molecular mechanisms that regulate cardiac A–P patterning.

MATERIALS AND METHODS

Zebrafish

Fish and embryos were maintained and staged as previously described (Westerfield, 1995). The mutations *casanova*^{ta56} (Chen *et al.*, 1996), *heart and soul*^{m129} (Stainier *et al.*, 1996), and *pandora*^{m313} (Stainier *et al.*, 1996) were originally generated by chemical mutagenesis and have been maintained by outcrossing heterozygous adults to standard wild-type strains. Homozygous mutant embryos were produced by mating adult heterozygotes; in general, the mutant phenotype was obvious in approximately 25% of the progeny, except as noted.

Identification of Myosin Genes

Oligonucleotide primers (5′-ATACAGGAGTTTAAGGAGGC-3′ and 5′-ACCAGTCTAATAAATCAAAAG-3′) were designed according to the sequences of available expressed sequence tags that resemble myosin genes (Chen *et al.*, 1998). Each primer was combined with a T7 primer to amplify 3′ gene fragments from a zebrafish adult heart cDNA library (generous gift of Dr. Roger Breitbart) phage suspension using conventional PCR techniques. Fragments were ligated into pGEM-T (Promega) for sequence analysis and riboprobe synthesis. GenBank accession numbers are AF114428 for *cardiac myosin light chain 2* and AF114427 for *ventricular myosin heavy chain.*

In Situ Hybridization

Whole-mount *in situ* hybridization was performed as previously described (Alexander *et al.*, 1998). All hybridizations were conducted at 70°C in a 65% formamide buffer. For transverse sections, stained embryos were fixed in 4% paraformaldehyde, embedded in JB4 (Polysciences), and sectioned at 5 μm. Photographs were taken using Kodak Ektachrome 160T film, a Leica MZ12 stereomicroscope, and a Zeiss Axioplan microscope; images were processed using Adobe Photoshop 4.0.

Immunofluorescence

Whole-mount immunofluorescence was performed as previously described (Stainier and Gilbert, 1990), using the monoclonal antibodies MF20 (Bader *et al.*, 1982) and S46 (generous gift of Dr. Frank Stockdale). The secondary reagents goat anti-mouse IgG1–FITC (fluorescein isothiocyanate) and goat anti-mouse IgG2b–TRITC (tetramethylrhodamine isothiocyanate) (Southern Biotechnology Associates) recognize S46 and MF20, respectively. Double-exposure photographs were taken using Fujichrome 1600 ASA film and a Zeiss Axioplan microscope; images were processed using Adobe Photoshop 4.0.

RESULTS

Identification of a Ventricle-Specific Myosin Heavy Chain Gene

Previous studies of cardiac chamber-specific myosin isoforms in chick and mouse have provided evidence for chamber-specific differentiation programs (Yutzey and

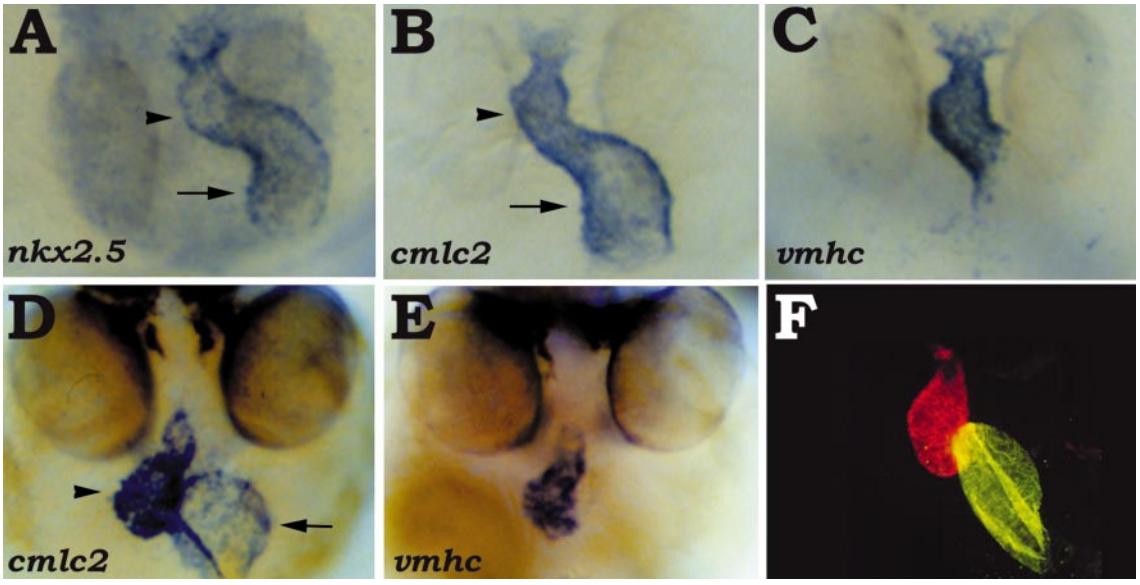

FIG. 1. The *vmhc* gene and S46 antigen are chamber-specific. (A, B, C) Dorsal views of 30-hpf embryos, anterior at the bottom; *in situ* hybridization showing *nkx2.5* (A), *cmlc2* (B), and *vmhc* (C) expression. While *nkx2.5* (A) and *cmlc2* (B) are expressed throughout both the ventricular (arrowhead) and the atrial (arrow) portions of the heart tube, *vmhc* (C) expression is restricted to the ventricular portion. (D, E) 48-hpf embryos viewed head-on, dorsal at the top; *in situ* hybridization with *cmlc2* (D) and *vmhc* (E) riboprobes. As the yolk is gradually absorbed, the ventricle (arrowhead) becomes rostral relative to the atrium (arrow). The expression of *cmlc2* (D) is maintained in both chambers, and the expression of *vmhc* (E) remains restricted to the ventricle. (F) Head-on view of a 48-hpf embryo stained with MF20 (TRITC) and S46 (FITC), dorsal at the top. In this double exposure, red fluorescence indicates MF20 staining of the ventricle, while yellow fluorescence indicates the overlap of S46 and MF20 staining in the atrium.

Bader, 1995; Lyons, 1994); we set out to identify similarly useful chamber-specific genes in zebrafish. Guided by available zebrafish expressed sequence tags (Chen *et al.,* 1998), we isolated fragments of several distinct myosin light and heavy chain genes. Two of these are discussed below: a regulatory myosin light chain gene, *cardiac myosin light chain 2* (*cmlc2*), and a myosin heavy chain gene, *ventricular myosin heavy chain* (*vmhc*).

In order to determine whether these genes are chamber-specific, we compared their expression to that of *nkx2.5,* a homeodomain transcription factor gene found throughout the embryonic myocardium (Fig. 1A; Chen and Fishman, 1996). By 30 h postfertilization (hpf), cardiac looping has placed the atrial/inflow portion of the zebrafish heart tube (Fig. 1A, arrow) distinctly to the left of the ventricular/outflow portion (Fig. 1A, arrowhead). At this stage, *cmlc2* is expressed uniformly throughout the myocardium, like *nkx2.5* (Figs. 1A and 1B). In contrast, *vmhc* is expressed only in the ventricular/outflow portion of the myocardium (Fig. 1C).

Restricted expression of *vmhc* persists after chamber demarcation is complete (Figs. 1D and 1E). By 48 hpf, the thick-walled, muscular ventricle (Fig. 1D, arrowhead) and the thin-walled atrium (Fig. 1D, arrow) are morphologically distinct. *cmlc2* is expressed throughout both chambers (Fig. 1D). In contrast, *vmhc* is expressed throughout the ventricle but not at all in the atrium (Fig. 1E); the posterior extent of *vmhc* expression coincides with the constriction at the atrioventricular boundary.

[It is important to note that the zebrafish heart tube first forms with its ventricular end positioned posteriorly and its atrial end tethered to the yolk sac anteriorly (Figs. 1A–1C). As development proceeds, the yolk is absorbed and the head rises dorsally, shifting the orientation of the heart tube into its final position (Stainier and Fishman, 1992), with the ventricle anterior and the atrium posterior (Figs. 1D–1F).]

The chamber-specific expression of *vmhc* provides the first example of a ventricle-specific gene in zebrafish. These data complement the previous demonstration that S46, a monoclonal antibody thought to recognize an atrium-specific myosin heavy chain isoform (Stainier and Fishman, 1992), is specific for the atrial myocardium at these stages (Fig. 1F; Alexander *et al.,* 1998). Thus, complementary regionalization of myosin heavy chain isoforms demonstrates discrete ventricular and atrial programs of gene expression in the zebrafish heart tube.

cmlc2 Is Expressed in Most, but Not All, nkx2.5-Expressing Cells

Given the restricted expression of *vmhc* relative to *cmlc2* within the heart, we proceeded to examine the early expres-

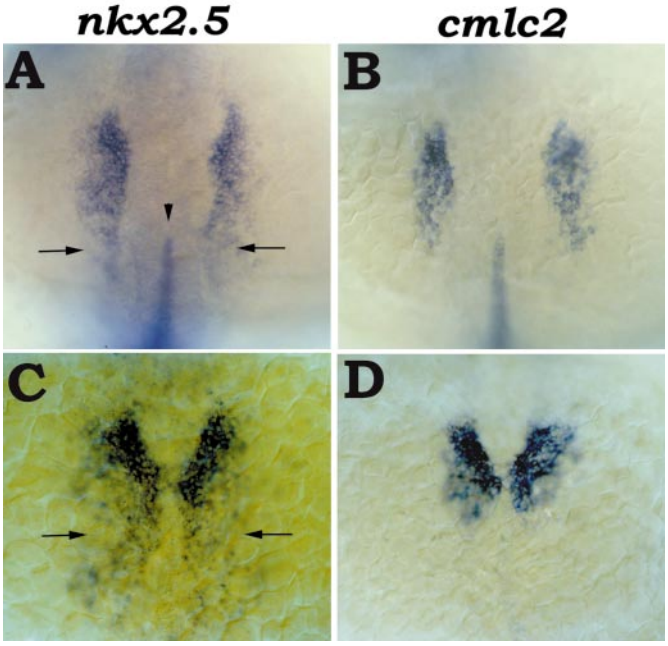

FIG. 2. *cmlc2* is expressed in most, but not all, *nkx2.5*-expressing cells. (A, B) Dorsal views of embryos at the 14-somite stage, anterior at the top; *in situ* hybridization with *nkx2.5* and *no tail* (A) or *cmlc2* and *no tail* (B) riboprobes. *no tail* is expressed in the developing notochord (Schulte-Merker *et al.*, 1994). (A) *nkx2.5* expression in bilateral stripes of precardiac mesoderm extends slightly (arrows) beyond the anterior tip of the developing notochord (shown by *no tail* expression, arrowhead). This most posterior region has relatively weak expression of *nkx2.5*. (B) The posterior boundaries of the bilateral stripes of *cmlc2* expression are aligned with the anterior tip of *no tail* expression. (C, D) Dorsal views of embryos at the 17-somite stage, anterior at the top; *in situ* hybridization with *nkx2.5* (C) or *cmlc2* (D) riboprobes. As the bilateral cardiac primordia bend toward each other, the most posterior *nkx2.5*-expressing cells (C, arrows) do not express *cmlc2* (D). Again, these most posterior cells express relatively weak levels of *nkx2.5* (C).

sion of these genes, hoping to identify informative subpopulations within the precardiac mesoderm. Since *nkx2.5* is the earliest known marker of zebrafish precardiac mesoderm (Chen and Fishman, 1996; Lee *et al.*, 1996), we compared the expression of *nkx2.5*, *cmlc2*, and *vmhc* prior to cardiac fusion.

First, we examined the early expression of *cmlc2* relative to *nkx2.5*. While expression of *nkx2.5* in precardiac mesoderm is clear at the initiation of somitogenesis (Chen and Fishman, 1996; Lee *et al.*, 1996), *cmlc2* expression is not apparent until the 13-somite stage (data not shown). *cmlc2* expression appears to be initiated in most, but not all, *nkx2.5*-expressing cells: a small posterior subset of *nkx2.5*-expressing cells do not express *cmlc2* (Figs. 2A and 2B). For example, at the 14-somite stage, the posterior boundary of *cmlc2* expression is aligned with the anterior boundary of the developing notochord (Fig. 2B), while *nkx2.5* expression extends posteriorly beyond the notochord tip (Fig. 2A). Similarly, at the 17-somite stage, as the bilateral cardiac primordia bow toward each other, the most posterior *nkx2.5*-expressing cells do not express *cmlc2* (Figs. 2C and 2D). These posterior *nkx2.5*$^+$ *cmlc2*$^-$ cells never appear to initiate *cmlc2* expression (data not shown) and likely correspond to a previously described posterior subpopulation of *nkx2.5*-expressing cells that does not contribute to the myocardium (Serbedzija *et al.*, 1998).

vmhc-Expressing Cells Are Located Medially within the Bilateral Regions of Precardiac Mesoderm

Having defined *cmlc2*$^+$ and *cmlc2*$^-$ subsets of *nkx2.5*-expressing cells, we proceeded to examine *vmhc* expression within the precardiac mesoderm. Like *cmlc2*, *vmhc* expression begins at the 13-somite stage (data not shown). From the time of its initiation, *vmhc* expression is restricted to a subset of *cmlc2*-expressing cells (Figs. 3A and 3B). While *cmlc2* expression is found in wide bilateral stripes of cells (Fig. 3A), the stripes of cells with intense *vmhc* expression are noticeably narrower (Fig. 3B) and appear to compose the most medial portion of each *cmlc2*-expressing region. As the cardiac primordia bend toward the midline, the medial restriction of *vmhc* expression is maintained (Figs. 3C and 3D). Transverse sections confirm the relationship between the *cmlc2*$^+$ and the *vmhc*$^+$ populations (Figs. 3E and 3F). At the 16-somite stage, the myocardial precursors form bilateral sheets just dorsal to the yolk syncytial layer (Lee *et al.*, 1996; Stainier *et al.*, 1993). While *cmlc2* expression extends throughout each bilateral sheet (Fig. 3E), *vmhc* expression is restricted to the most medial cells within each sheet (Fig. 3F).

The existence of two distinct subsets of *cmlc2*-expressing cells—medial/*vmhc*$^+$ and lateral/*vmhc*$^-$—at the 15-somite stage represents the earliest molecular diversification detected within the bilateral regions of precardiac mesoderm in zebrafish. Moreover, if these medial *vmhc*-expressing cells (Figs. 3B, 3D, and 3F) are in fact the precursors of the *vmhc*-expressing cells in the ventricle (Figs. 1C and 1E), then these data would also provide the first molecular evidence in support of specification of chamber-specific lineages prior to cardiac fusion in zebrafish.

Following cmlc2 and vmhc Expression during Heart Tube Assembly

To test the hypothesis that the medially located *cmlc2*$^+$ *vmhc*$^+$ cells are the precursors of the ventricular myocardium, we followed the relative locations of *cmlc2*-expressing and *vmhc*-expressing populations throughout the process of heart tube assembly, examining embryos at regular and frequent intervals between the 15-somite stage (16.5 hpf) and 26 hpf. Below, we summarize the major findings from these efforts, highlighting a few particularly

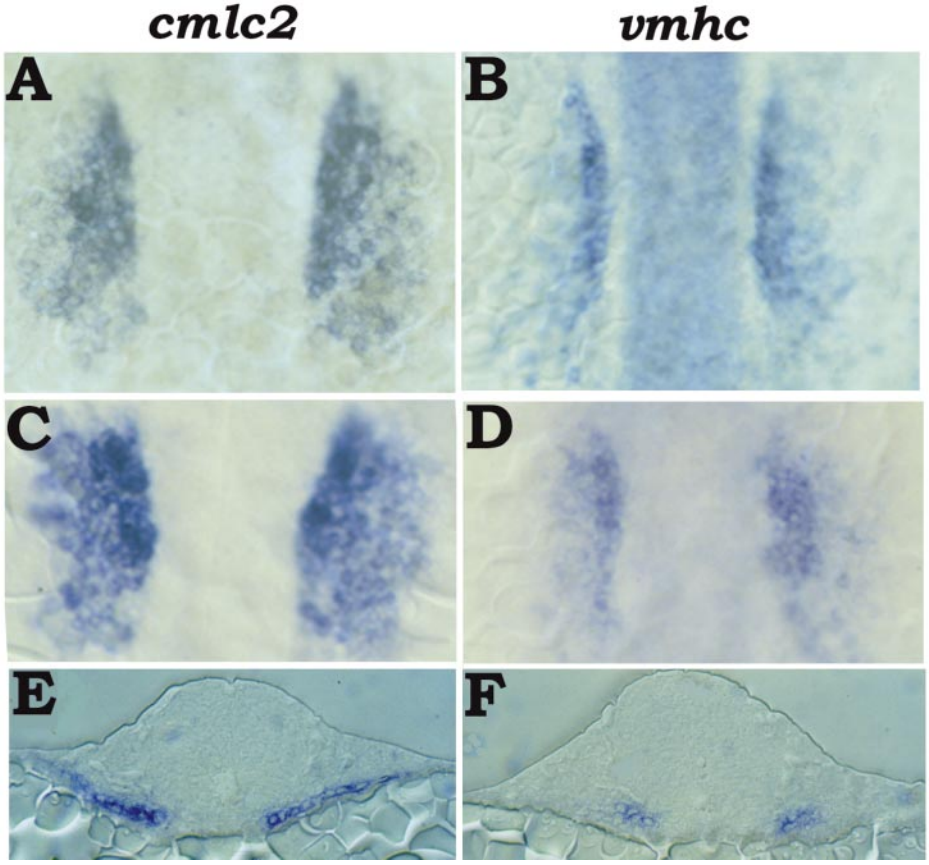

FIG. 3. *vmhc* expression is restricted to a subset of *cmlc2*-expressing cells. (A, C, E) Expression of *cmlc2*. (B, D, F) Expression of *vmhc*. (A, B) Dorsal views of embryos at the 15-somite stage, anterior at the top. More precardiac cells express *cmlc2* (A) than *vmhc* (B); intentional overstaining of the embryo in (B) demonstrates that intense *vmhc* expression appears only in the most medial myocardial precursors. In addition to expression in precardiac cells, *vmhc* is also expressed in the somites (data not shown). (C, D) Dorsal views of embryos at the 16-somite stage, anterior at the top. Again, *vmhc* expression (D) appears restricted to the most medial *cmlc2*-expressing cells (C). (E, F) Transverse sections of 16-somite stage embryos also demonstrate that the *vmhc*-expressing cells (F) are a medial subset of the *cmlc2*-expressing cells (E).

informative stages (Fig. 4). These data provide a model for the process by which the medial $cmlc2^+$ $vmhc^+$ populations could come together to create the ventricle.

Being the most medial of the myocardial precursors, the *vmhc*-expressing cells compose the leading edge as the bilateral $cmlc2^+$ sheets migrate toward the midline (Figs. 3A–3D and 4A and 4B). As they approach, the two populations bend toward one another, first making contact through a thin bridge of cells slightly posterior to their A–P midpoint (Fig. 4A, arrowhead). The cells that form this bridge as well as the rest of the medial section of this butterfly-shaped configuration express *vmhc* (Fig. 4B), consistent with the prior medial position of $vmhc^+$ cells.

Following this initial contact, the bilateral sheets proceed to fuse. The portions posterior to the bridge fuse first (data not shown; see Fig. 7E for an example), followed by an anterior closure that creates a central lumen. Viewed dorsally, the $cmlc2^+$ cells appear to form a simple ring (Fig. 4C); however, the structure is actually a shallow cone (Stainier *et al.*, 1993). The apex of this cone is raised dorsally around the lumen (Stainier *et al.*, 1993) and is composed of *vmhc*-expressing cells (Fig. 4D).

Next, the cardiac cone is transformed into a linear tube. The process begins when the apex of the cone tilts posteriorly and toward the right, shifting the cone's axis from a dorsal–ventral (D–V) plane to an A–P plane (Figs. 4E and 4F; and data not shown). The apex thus appears to establish the ventricular/outflow end of the nascent heart tube (Fig. 4F). During tilting, the lumen of the cone is preserved, although it is not visible when viewed dorsally (Figs. 4E and 4F and data not shown).

Following the initial movements of the apex, the cells that compose the wide base of the cone appear to gradually coalesce into a tube (Fig. 4G). In the example shown, the

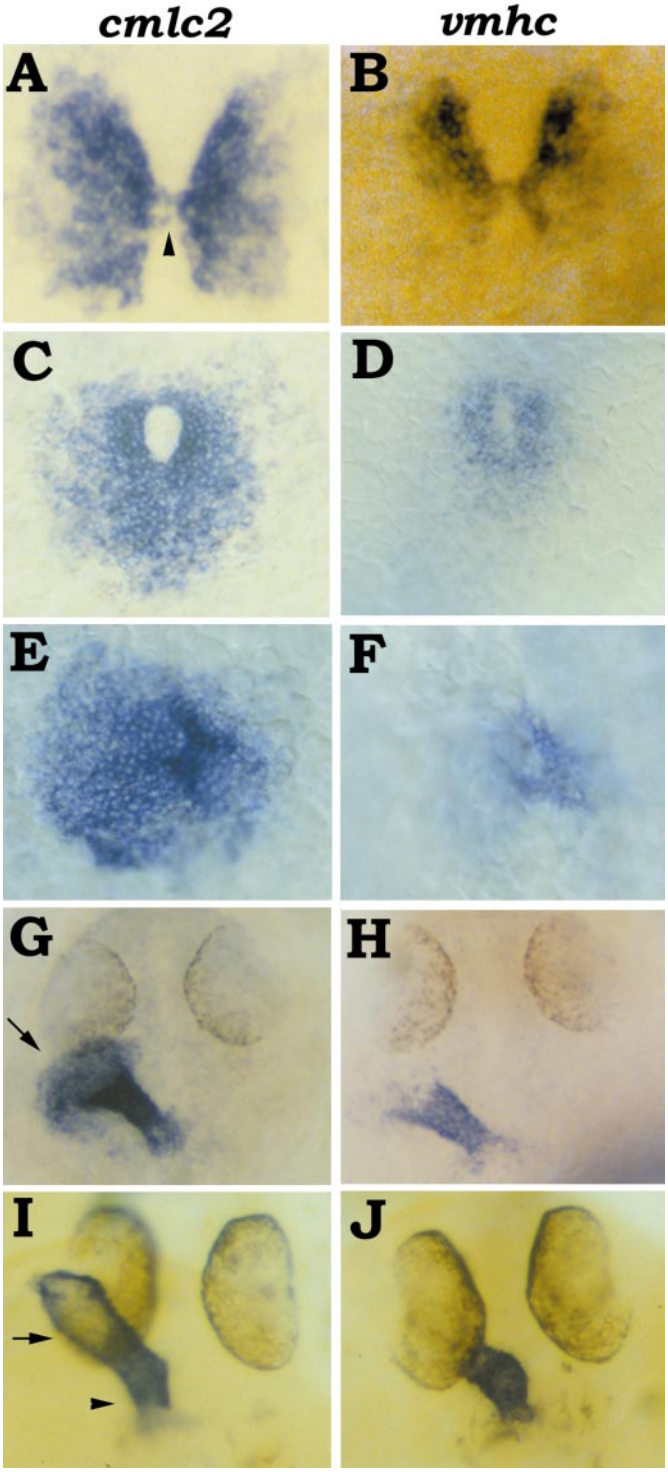

FIG. 4. Following *cmlc2* and *vmhc* expression during heart tube assembly. (A, C, E, G, I) Expression of *cmlc2*. (B, D, F, H, J) Expression of *vmhc*. All panels show dorsal views, anterior at the top. (A, B) 18-somite stage; the myocardial precursors (A) make contact via a bridge (arrowhead) of *vmhc*-expressing cells (B). (C, D) 21-somite stage; the cardiac cone (C) forms with *vmhc*-expressing cells (D) at its center and apex. (E, F) 23-somite stage; the cardiac cone (E) begins its transformation into a tube with the extension and tilting of the *vmhc*-expressing apex (F). (G, H) 24 hpf; as tube formation continues (G), the ventricular end (H) is nearly completely assembled while the atrial precursors (arrow in G) are still coalescing. (I, J) 26 hpf; the heart tube (I) expresses *vmhc* only within the future ventricle (J), while both the future ventricle (arrowhead in I) and the future atrium (arrow in I) express *cmlc2*.

ventricular portion of the tube appears complete and formation of the atrium has begun (Figs. 4G and 4H). The conversion from cone to tube is most likely accompanied by some myocardial proliferation, since the number of *vmhc*-expressing cells increases (compare Figs. 4F and 4H). When heart tube assembly is complete, *vmhc*-expressing cells form the ventricular/outflow portion, while the myocardial cells of the atrial/inflow portion express only *cmlc2* (Figs. 4I and 4J).

The careful examination of *cmlc2* and *vmhc* expression patterns cannot formally distinguish whether changes in expression reflect a complex series of cellular movements or a rapid series of dramatic changes in gene regulation. Nevertheless, based on examination of a large number of embryos and timepoints (Figs. 3 and 4; and data not shown), we favor the interpretation that these data represent the relative movements of the *cmlc2*-expressing and *vmhc*-expressing populations and strengthen the conjecture that the $cmlc2^+$ $vmhc^+$ cells located medially within the precardiac mesoderm are ventricular precursors. For convenience, we will refer to $cmlc2^+$ $vmhc^+$ cells as presumed ventricular precursors and $cmlc2^+$ $vmhc^-$ cells as presumed atrial precursors, with the understanding that these assignments involve interpretive assumptions.

Achievement of Cardiac A–P Pattern Does Not Require Cardiac Fusion

The relationships between *cmlc2*-expressing and *vmhc*-expressing populations suggest how cardiac fusion could facilitate the conversion of a medial–lateral (M–L) pattern into an A–P pattern (Fig. 4). Several zebrafish mutations prohibit cardiac fusion, resulting in bilateral beating "hearts," a condition called cardia bifida (Alexander *et al.*, 1998; Chen *et al.*, 1996; Stainier *et al.*, 1996). Intriguingly, proper cardiac A–P patterning is possible in these mutant embryos; for example, embryos homozygous for the zebrafish mutation *casanova* (*cas*) (Chen *et al.*, 1996) have two lateral hearts, each with an anterior ventricle and a posterior atrium (Fig. 5A). To understand how this normal A–P patterning could occur, we investigated the relative orientation of the presumed ventricular and atrial precursors in *cas* mutant embryos; similar results were obtained with several other cardia bifida mutants (data not shown).

Homozygous *cas* mutants cannot be distinguished from their wild-type siblings by virtue of differences in *cmlc2* or

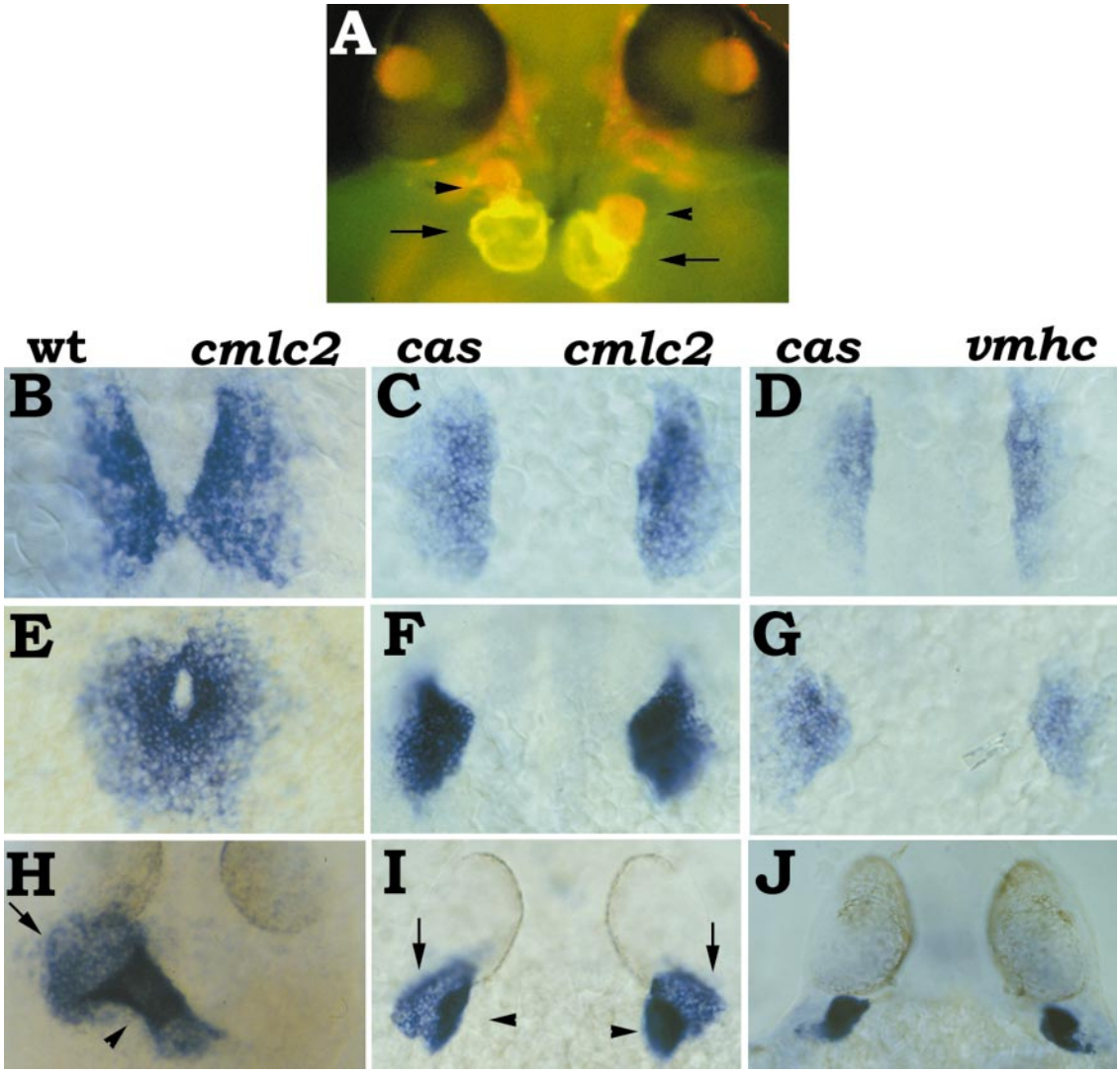

FIG. 5. Achievement of cardiac A–P pattern does not require cardiac fusion. (A) Ventral view of a 48-hpf *casanova* (*cas*) mutant embryo stained with MF20 (TRITC) and S46 (FITC), anterior at the top. Red fluorescence indicates MF20 staining of ventricular tissue (arrowheads) in the anterior portion of each lateral heart, while yellow fluorescence indicates the overlap of S46 and MF20 staining in atrial tissue (arrrows) in the posterior portion of each lateral heart. Staining of eye musculature with MF20 is also apparent just medial to each eye. (B–J) Dorsal views, anterior at the top, of wild-type and *cas* mutant embryos. (B, E, H) Expression of *cmlc2* in wild-type embryos. (C, F, I) Expression of *cmlc2* in *cas* mutant embryos. (D, G, J) Expression of *vmhc* in *cas* mutant embryos. (B, C, D) 18-somite stage; while cardiac fusion begins in wild-type embryos (B), the myocardial precursors in mutant embryos (C) remain stationary. *vmhc*-expressing cells in mutant embryos are located medially (D). (E, F, G) 21-somite stage; while the cardiac cone forms in wild-type embryos (E), myocardial precursors in mutant embryos (F) bend slightly toward the midline, led by *vmhc*-expressing cells (G). (H, I, J) 24 hpf; as a tube forms in wild-type embryos (H), myocardial precursors in mutant embryos (I) appear to form modified cones, with *vmhc*-expressing cells leading the way (J). In both wild-type (H) and mutant (I) embryos, there is an apparent condensation of preventricular tissue (arrowheads) while preatrial tissue (arrows) remains more diffuse.

vmhc expression until the 18-somite stage, when the myocardial precursors normally begin fusion (Fig. 5B). At this stage, mutant embryos are conspicuous, as their myocardial precursors remain stationary (Figs. 5C and 5D). Notably, the specification of the presumed ventricular precursors in *cas* mutants seems normal: the M–L pattern of gene expression is intact (Figs. 5C and 5D). As cardiac fusion and heart tube assembly proceed in wild-type embryos, the bilateral populations of myocardial precursors in *cas* embryos seem to exhibit behaviors similar to those of their wild-type counterparts. For example, while the cardiac cone forms in wild-type embryos (Fig. 5E), the mutant myocardial precur-

sors bow slightly toward the midline, led by *vmhc*-expressing cells (Figs. 5F and 5G). As the wild-type tube coalesces (Fig. 5H), the forming ventricle appears denser than the extended sheet of atrial precursors (also see Figs. 4G and 4H). Similarly, complex cellular movements in mutant embryos position the dense ventricular precursors posterior to a sheet of atrial precursors (Figs. 5I and 5J). Ultimately, each bifid heart appears to form a tube (data not shown) and, as in normal embryos (Fig. 1F), the yolk regresses, swinging each atrium into a posterior position (Fig. 5A). Based on this analysis, we conclude that achievement of a normal cardiac A–P pattern does not require cardiac fusion.

The heart and soul Mutation Blocks Heart Tube Assembly at an Intermediate Stage

While cardiac A–P patterning is not dependent on cardiac fusion, the process of cardiac fusion surely plays an integral role during the assembly of a patterned heart tube in wild-type embryos. Even so, the achievement of cardiac fusion does not necessarily ensure the proper A–P orientation of the ventricle and atrium. This is demonstrated by the *heart and soul* (*has*) mutation, which was originally described as causing a "small heart" (Stainier *et al.,* 1996). In fact, the small, dense nature of the *has* heart is not due to a reduced amount of myocardium (data not shown), but rather to a gross malformation of the heart tube. The atrium, which lies posterior to the ventricle in the wild-type heart (Fig. 6A), surrounds the ventricle in the *has* heart (Figs. 6B and 6C; Fishman and Chien, 1997).

This aberrant orientation of the atrium with respect to the ventricle could be the result of an early disruption of the M–L organization of the myocardial precursors. Alternatively, initial M–L patterning could be normal and the mutation might instead disrupt a morphogenetic process independent of the proper specification of ventricular and atrial lineages. To distinguish between these two possibilities and identify the point at which heart tube morphogenesis goes awry in *has* mutants, we followed the expression of *cmlc2* and *vmhc* during heart tube assembly.

In homozygous *has* mutants, the myocardial precursors migrate toward the midline in a normal manner and fuse to form the cardiac cone (Figs. 6D, 6E, and 6F). At the 23-somite stage, however, when the apex of the cone normally tilts to allow for the elongation of the heart tube (Fig. 6G), the *has* cone remains stationary (Figs. 6H and 6I). The mutant heart retains a cone-like structure, but becomes increasingly dysmorphic throughout the time that the more lateral regions of the cone are coalescing into a tube in wild-type siblings (Figs. 6J, 6K, and 6L). In time, the atrial precursors that make up the wide base of the *has* cone fold back over the ventricular precursors in the apex, resulting in the atrium being inside-out over the ventricle (Figs. 6B and 6C).

These data suggest that the abnormal chamber orientation in *has* mutants is unlikely to be caused by improper specification of ventricular and atrial lineages, as *cmlc2* and *vmhc* expression are normal through the formation of the cardiac cone (Figs. 6D, 6E, and 6F; and data not shown). Instead, the *has* mutation blocks heart tube assembly at an intermediate stage. *has* function appears to be required for the tilting of the cone that normally facilitates the conversion of the M–L pattern of the myocardial precursors into the A–P pattern of the heart tube.

The pandora Gene is Required for Early vmhc Expression

The genes *cas* and *has* are both critical for the assembly of a single midline heart tube with the proper A–P orientation. However, neither of these genes appears to play a role in the initial diversification of the myocardial precursors. The zebrafish mutation *pandora* (*pan*) causes a number of embryonic defects, including a notable deficiency of ventricular tissue (Stainier *et al.,* 1996); we examined the impact of the *pan* mutation on early *cmlc2* and *vmhc* expression.

The heart of a homozygous *pan* mutant contains only a thin stalk of ventricle-like tissue, in contrast to the muscular anterior chamber of a wild-type sibling (compare Figs. 7A and Fig. 1F); this stalk is attached to the anterior end of a bulbous atrium–like chamber that is recognized by the S46 atrial-specific antibody (Fig. 7A) While the *pan* "ventricle" does not contract normally (data not shown), these anterior myocardial cells do express both *cmlc2* and *vmhc* robustly (Figs. 7B, 7C, and 7D). Thus, the A–P orientation of the *pan* heart is relatively normal, with a $cmlc2^{+}$ $vmhc^{+}$ population positioned anterior to a $cmlc2^{+}$ $vmhc^{-}$ population; even so, the *pan* mutation clearly disrupts ventricular development.

Both *cmlc2* expression and *vmhc* expression are affected in *pan* mutants at an earlier stage. It is difficult to detect any *cmlc2* expression in *pan* embryos prior to the 18-somite stage (data not shown). At the 18-somite stage, when cardiac fusion begins in wild-type embryos (Fig. 7E), *pan* embryos exhibit relatively faint and thin bilateral stripes of *cmlc2* expression (Fig. 7F) and lack *vmhc* expression (Fig. 7G). By the 21-somite stage, when cone formation occurs in wild-type embryos (Fig. 7H), bilateral *cmlc2* expression becomes slightly stronger in *pan* embryos (Fig. 7I). At this stage, faint *vmhc* expression can be detected in some *pan* embryos (Fig. 7J), although the intensity of expression as well as the number of *vmhc*-expressing cells is variable (data not shown). Anterior closure of the cardiac cone rarely proceeds normally in *pan* embryos (data not shown), but a modified cone does form (Fig. 7K); the base of the *pan* cone is especially wide and frequently appears to be split (compare Figs. 4E and 7K), and the apex of the *pan* cone expresses *vmhc* (Fig. 7L). This cone extends and the *pan* myocardium comes to resemble an inverted goblet composed of a ventricular stem and an atrial cup (Figs. 7C and 7D).

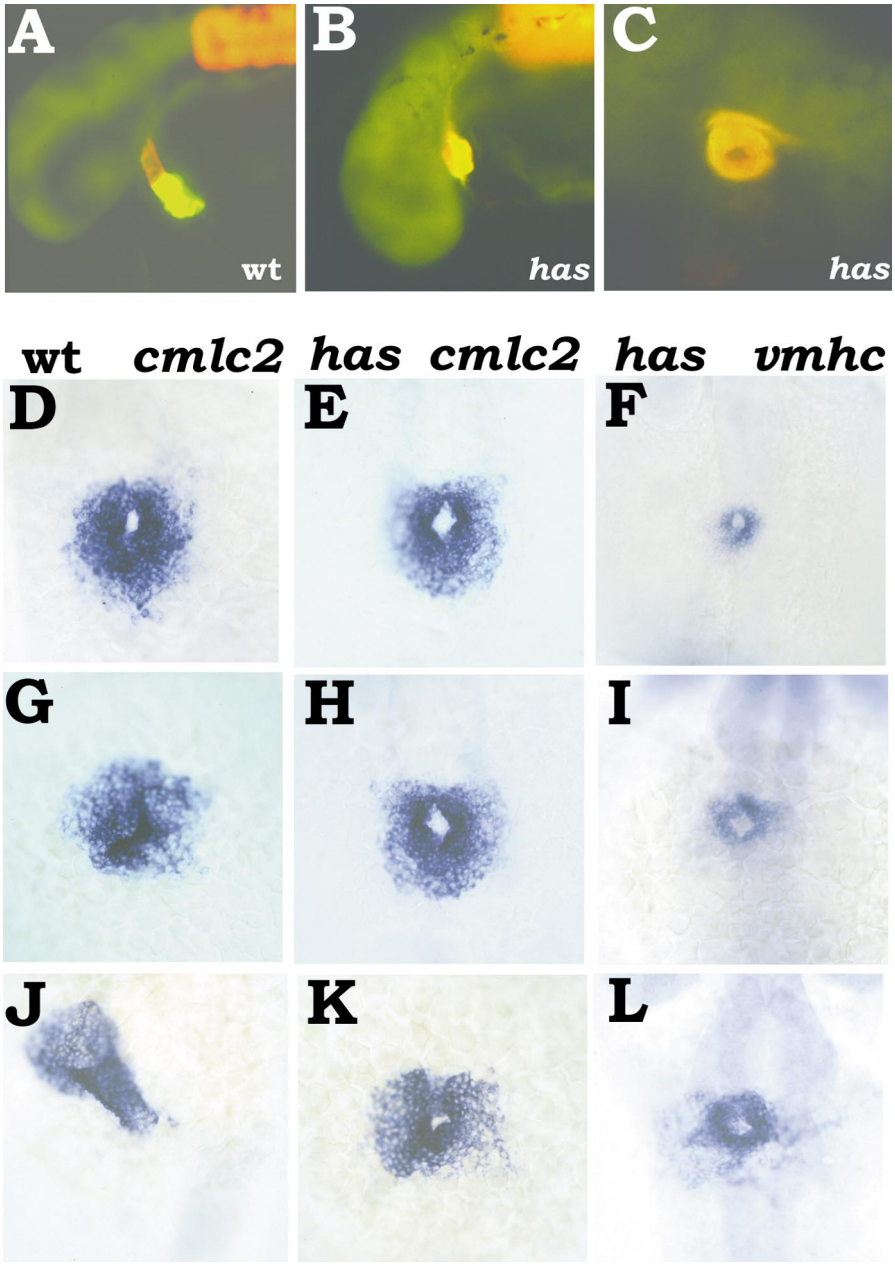

FIG. 6. *heart and soul* (*has*) disrupts heart tube assembly at an intermediate stage. (A, B, C) 27-hpf embryos stained with MF20 (TRITC) and S46 (FITC), anterior to the left. Red fluorescence indicates MF20 staining of ventricular tissue, while yellow fluorescence indicates the overlap of S46 and MF20 staining in atrial tissue. (A) Lateral view of wild-type embryo. The atrium (yellow) lies posterior to the ventricle (red). (B) Lateral view of *has* mutant. (C) Ventral view of *has* mutant. The atrium (yellow) surrounds the ventricle (red). (D–L) Dorsal views, anterior at the top, of wild-type and *has* mutant embryos. (D, G, J) Expression of *cmlc2* in wild-type embryos. (E, H, K) Expression of *cmlc2* in *has* mutant embryos. (F, I, L) Expression of *vmhc* in *has* mutant embryos. (D, E, F) 21-somite stage; the cardiac cone has formed and *has* mutants are indistiguishable from their wild-type siblings. (G, H, I) 23-somite stage; while the apex of the cone has tilted in wild-type embryos (G), the cone in *has* mutants remains stationary (H, I). (J, K, L) 24 hpf; the *has* heart still retains a cone-like structure (K, L), even as formation of the wild-type heart tube is nearly complete (J).

These data indicate that *pan* function is essential for the robust and timely expression of both *cmlc2* and *vmhc* at early stages; *vmhc* expression appears to be more dependent on *pan* function than *cmlc2* expression is (Figs. 7E–7J). Cardiac fusion and heart tube assembly are also delayed and aberrant in *pan* mutants (Figs. 7E–7L); these defects could

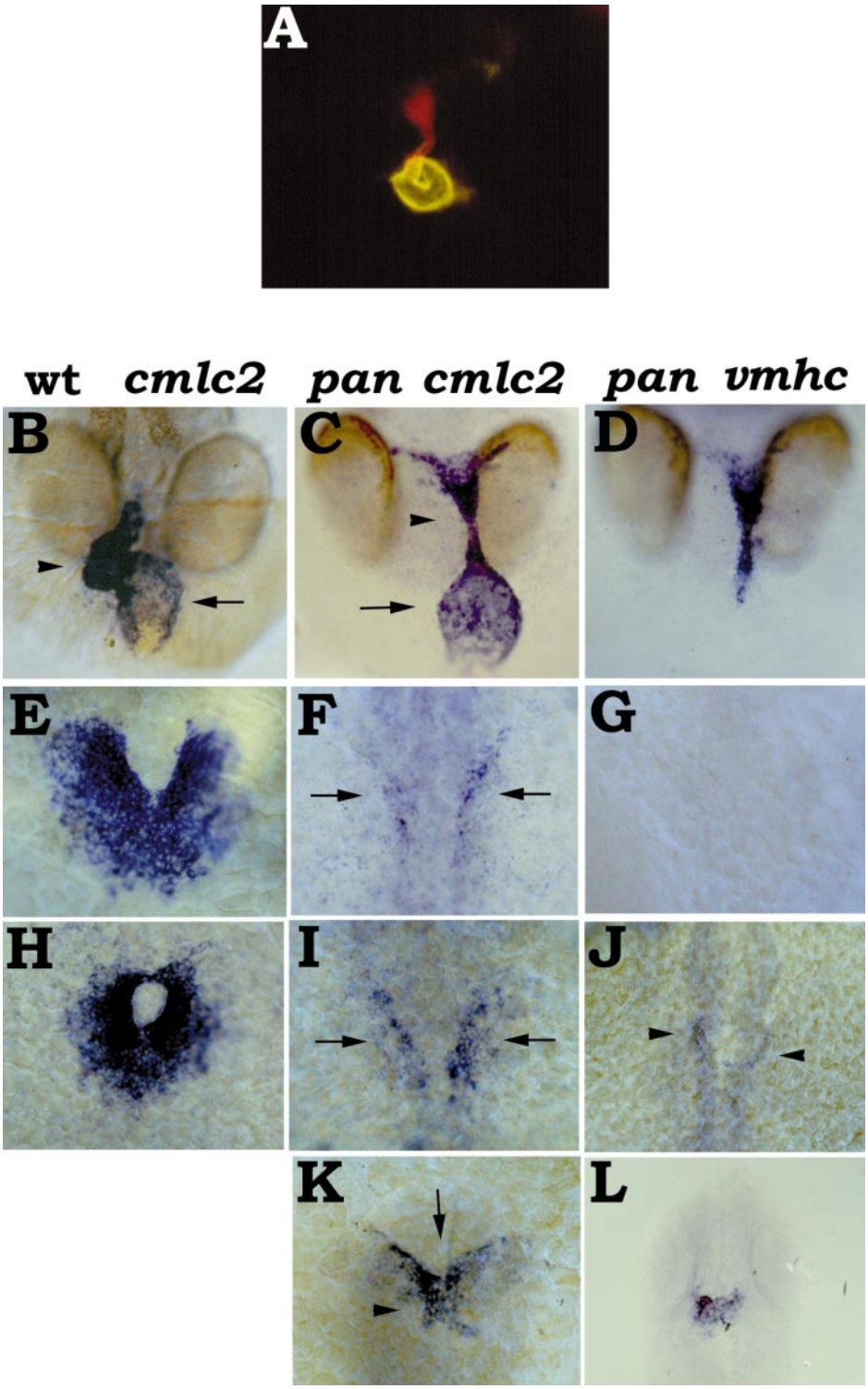

FIG. 7. The *pandora* (*pan*) mutation affects ventricle formation as well as early expression of *cmlc2* and *vmhc*. (A) Head-on view of a 48-hpf *pan* mutant embryo stained with MF20 (TRITC) and S46 (FITC), dorsal at the top. A thin stalk of ventricular tissue (red) is attached to the rostral end of a bulbous atrium (yellow). (B, E, H) Expression of *cmlc2* in wild-type embryos. (C, F, I, K) Expression of *cmlc2* in *pan* mutant embryos. (D, G, J, L) Expression of *vmhc* in *pan* mutant embryos. (B–D) Head-on views, dorsal at the top, of 48-hpf embryos. In *pan* mutants, the heart is composed of a bulbous atrium (C, arrow) and a thin stalk of ventricular tissue (C, arrowhead). (E–L) Dorsal views,

simply be consequences of the poor early differentiation and patterning of the myocardial precursors.

DISCUSSION

The identification of *cmlc2* and *vmhc* has facilitated several new insights into the process of assembling a patterned heart tube. The restricted expression of *vmhc* relative to *cmlc2* reveals the existence of two discrete subpopulations of myocardial precursors from an early stage; these may represent the ventricular and atrial precursors. The expression patterns of *cmlc2* and *vmhc* during the process of heart tube assembly provide the basis for a compelling model to describe the relative movements of the presumed cardiac chamber primordia in wild-type embryos. By examining *cmlc2* and *vmhc* expression in *casanova* and *heart and soul* mutants, we demonstrate that, even though cardiac A–P patterning does not depend on cardiac fusion, the successful completion of cardiac fusion does not necessarily guarantee the proper A–P orientation of the chambers. Finally, our data indicate that *pandora* function is critical for the initial establishment of $cmlc2^{+}$ $vmhc^{+}$ and $cmlc2^{+}$ $vmhc^{-}$ populations of myocardial precursors.

Differentiation of Precardiac Mesoderm into Two Populations of Myocardial Precursors Occurs Prior to Cardiac Fusion

Although *nkx2.5* is often considered a marker of zebrafish precardiac mesoderm (Chen and Fishman, 1996; Lee *et al.*, 1996), not all *nkx2.5*-expressing cells contribute to the myocardium (Goldstein and Fishman, 1998; Serbedzija *et al.*, 1998). Specifically, of the cells that express *nkx2.5* at the 14-somite stage, only those that lie beside the prechordal plate seem to be myocardial precursors (Serbedzija *et al.*, 1998). *cmlc2* expression is restricted to this subset of *nkx2.5*-expressing cells (Fig. 2), thereby providing molecular evidence that myocardial differentiation is under way in a distinct group of *nkx2.5*-expressing cells by this stage.

Medial ($cmlc2^{+}$ $vmhc^{+}$) and lateral ($cmlc2^{+}$ $vmhc^{-}$) subsets of myocardial precursors may represent discrete preventricular and preatrial lineages (Fig. 3). Our extended analyses of *cmlc2* and *vmhc* expression patterns (Fig. 4) are consistent with this hypothesis, assuming that it is reasonable to deduce cell movements by inspecting gene expression at multiple timepoints. In this case, our data would indicate that cardiac A–P patterning—that is, the specification and differentiation of future anterior/ventricular and posterior/atrial lineages—precedes cardiac fusion in zebrafish. Fate mapping experiments will be required to prove that ventricular precursors are located more medially than atrial precursors at the 15-somite stage.

The distinct M–L organization of the presumed ventricular and atrial precursors in zebrafish is an interesting contrast to the proposed A–P organization previously suggested by fate maps and explant analyses in chick (DeHaan, 1965; Stalsberg and DeHaan, 1969; Satin *et al.*, 1988; Yutzey *et al.*, 1995). These seemingly disparate arrangements may actually be quite similar. While the zebrafish cardiac cone forms via a medial fusion (Fig. 4), the chick cardiac crescent seems to form from two bilateral regions of precardiac mesoderm that come together at their anterior ends (DeHaan, 1965; Stalsberg and DeHaan, 1969). Thus, it seems that cardiac chamber primordia in both chick and fish, and perhaps in all vertebrates, are positioned such that cardiac fusion begins with the assembly of the ventricle.

The Relationship Between Cardiac A–P Patterning and Cardiac Fusion

Our analyses of *cmlc2* and *vmhc* expression throughout cardiac fusion and heart tube assembly provide new resolution of these dynamic and poorly understood processes (Fig. 4). In particular, these data demonstrate that *vmhc*-expressing cells are always at the vanguard of heart formation: they form the leading edge of the migrating precardiac mesoderm, the apex of the cardiac cone, and the initial foundation of the heart tube.

Given our new perspective on the complex movements required to transform the cardiac cone into the linear heart tube, it is exciting to learn that the *has* mutation specifically disrupts this process (Fig. 6). The tilting of the cone's apex, which does not occur in *has* mutants, is normally a crucial step in converting the early M–L pattern of the myocardial precursors into the A–P pattern of the heart tube. It is not yet known how *has* controls the tilting of the

anterior at the top. (E, F, G) 18-somite stage; *pan* embryos exhibit relatively faint and thin bilateral stripes of *cmlc2*-expressing cells (F, arrows), in contrast to the robust *cmlc2*-expressing population of fusing myocardial precursors in wild-type siblings (E). *pan* embryos do not express *vmhc* at this stage (G). (H, I, J) 21-somite stage; *pan* embryos exhibit slightly stronger *cmlc2* expression (I, arrows), but still far less than in wild-type embryos (H). Some *pan* embryos have faint bilateral patches of *vmhc* expression (J, arrowheads). (K, L) 36 hpf; cardiac cone formation is delayed and abnormal in *pan* mutants (K). Often, *pan* mutant cones have a split base (K, arrow). The apex of the *pan* cone (K, arrowhead) expresses a significant amount of *vmhc* (L). It is important to note that *pan* embryos lag behind their wild-type siblings during somitogenesis. For example, *pan* embryos usually have only 16 somites when their wild-type siblings have 20 somites. In (E–G) and (H–J), we are comparing *pan* embryos with wild-type embryos with the same number of somites; i.e., the wild-type siblings are fixed a few hours before the *pan* mutants. Also note that the precise morphology of the developing myocardium in *pan* mutants can vary; these examples represent typical expression patterns observed in a majority of mutants.

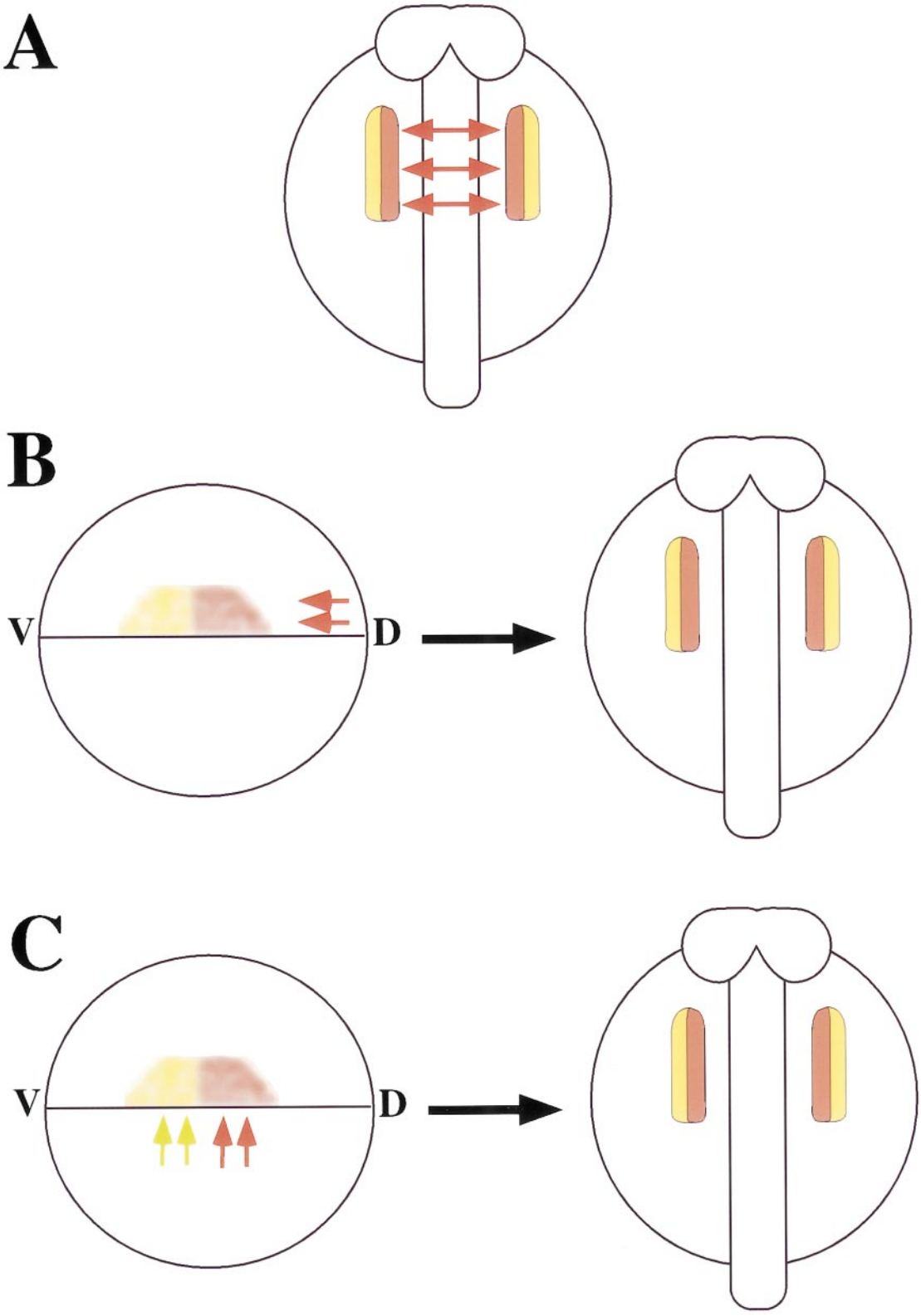

FIG. 8. Models for the specification of distinct ventricular and atrial lineages. (A–C) Red indicates ventricular precursors, yellow indicates atrial precursors, and red or yellow arrows represent hypothetical signals that regulate the specification of ventricular or atrial lineages, respectively. (A) Schematic dorsal view of a 15-somite stage embryo. Signals (red arrows) emanating from the midline may be responsible

cone; it may affect intrinsic characteristics of the myocardium or extrinsic forces involved in tilting. The identification of the *has* gene will allow the future dissection of tilting morphogenesis at the molecular level.

Despite the involvement of the cardiac cone in the normal transition between a M–L pattern and an A–P pattern, the achievement of a proper cardiac A–P pattern does not require cardiac fusion, as demonstrated by *cas* mutants (Fig. 5). Even when the bilateral populations of myocardial precursors never meet, characteristics intrinsic to each separate region evidently allow adjustments similar to those seen in wild-type embryos, ultimately creating an A–P pattern within each lateral heart. Future real-time comparisons of the movements of $cmlc2^{+}$ $vmhc^{+}$ and $cmlc2^{+}$ $vmhc^{-}$ cells in wild-type and *cas* mutant embryos should advance our comprehension of how an A–P pattern is created in the absence of cardiac fusion.

pandora Affects Cardiac Patterning Prior to Cardiac Fusion

While studies of *cas* and *has* mutants have enriched our understanding of the relationship between cardiac patterning and cardiac fusion, they have not uncovered the mechanisms responsible for the early M–L patterning of myocardial precursors. In contrast, the *pan* mutation provides a compelling point of entry for the analysis of early cardiac patterning events, especially the specification of the presumed ventricular precursors.

pan mutant embryos do not express detectable levels of *vmhc* until many hours after *vmhc* expression is initiated in wild-type embryos (Figs. 7G and 7J). When a few *vmhc*-expressing cells are finally apparent in *pan* embryos, they express lower levels of *vmhc* than their wild-type counterparts (Fig. 7J). Nevertheless, the *vmhc*-expressing cells in older *pan* embryos (>30 hpf) exhibit robust levels of *vmhc* message (Figs. 7D and 7L). In the absence of *pan* function, myocardial cells may struggle to become competent to express *vmhc*. Alternatively, *vmhc* expression may be controlled differently at different stages, possibly in a *pan*-dependent fashion prior to cardiac fusion and in a *pan*-independent fashion following cardiac fusion.

pan mutants also have difficulty with the development of the presumed atrial precursors (Fig. 7). Robust *cmlc2* expression is delayed and there seem to be a reduced number of $cmlc2^{+}$ $vmhc^{-}$ cells in *pan* embryos. While these defects are not as dramatic as the ventricular defects, we conclude that *pan* influences general myocardial differentiation in addition to the specification of ventricular precursors.

The compound role of *pan* during early myocardial differentiation and patterning could be explained in several ways. For example, the genetic pathway regulating general myocardial differentiation may share molecular components, such as the *pan* gene product, with the genetic pathway regulating ventricular specification. Alternatively, *pan* may function in the specification of both ventricular and atrial precursors, with a more critical role in ventricular precursors. Additionally, the defects in cardiac patterning could be secondary to the defects in myocardial differentiation: perhaps the health or abundance of properly differentiating myocardial tissue is a requirement for successful ventricular specification. While we cannot yet distinguish between these possibilities, we suspect that the processes of early myocardial differentiation and patterning are tightly interrelated. Our preliminary analyses of a number of mutations affecting ventricular development (Alexander *et al.,* 1998; Chen *et al.,* 1996; Stainier *et al.,* 1996) suggest a trend in which mutations—like *pan*—that affect early *vmhc* expression also affect general myocardial differentiation and the execution of efficient cardiac fusion (data not shown).

Future studies should shed light on the involvement of *pan* in myocardial differentiation and patterning. In particular, it will be important to determine whether the myocardial requirement for *pan* function is cell-autonomous. Furthermore, the identification of the *pan* gene is likely to be a crucial advance in our understanding of cardiac A–P patterning, since very few molecules have been implicated in the early stages of this process. Previous studies have focused on the ability of exogenous retinoic acid (RA) treatments to inhibit ventricular development in zebrafish, chick, and mouse embryos (Stainier and Fishman, 1992; Yutzey *et al.,* 1994, 1995; Xavier-Neto *et al.,* 1999; Chazaud *et al.,* 1999), suggesting that endogenous retinoids encourage atrial development, potentially through the control of *hox* gene expression (Searcy and Yutzey, 1998). In fact, recent analyses have demonstrated that localized synthesis of RA within preatrial regions of the murine heart tube is essential for the regionalization of RA activity and the differentiation of the atrium (Moss *et al.,* 1998; Niederreither *et al.,* 1999; Xavier-Neto *et al.,* 1999). Thus, one role of RA is evidently downstream of an initial A–P pattern that

for the specification of ventricular precursors in the medial portion of the precardiac mesoderm. (B) On the left, schematic lateral view of a zebrafish blastula at the initiation of gastrulation; dorsal is to the right, the upper hemisphere represents the blastoderm, and the lower hemisphere represents the yolk. On the right, schematic dorsal view of a 15-somite stage embryo as in (A). Signals (red arrows) emanating from the dorsal gastrula organizer may be responsible for the specification of ventricular precursors in the dorsal portion of the precardiac field. Following gastrulation, these cells would come to reside medially within the precardiac mesoderm. (C) Schematic views as in (B). Early specification of ventricular and atrial lineages within the blastula may be influenced by a prepattern within the extraembryonic yolk syncytial layer. Translation of this pattern to the blastula (represented by red and yellow arrows) may differentially induce the ventricular and atrial lineages.

functions to restrict the myocardial expression of RA-synthesizing enzymes; it will be interesting to determine the relationship of *pan* and the synthesis of endogenous retinoids. Additionally, it will be important to determine the interactions of *pan* and *irx4*, a transcription factor involved in the control of ventricular differentiation in chick (Bao *et al.*, 1999).

M–L Orientation of Presumed Ventricular and Atrial Primordia Suggests New Models for Cardiac Patterning

The *cmlc2* and *vmhc* expression patterns inspire new hypotheses regarding the molecular mechanisms responsible for cardiac chamber specification. For example, the medial location of $cmlc2^{+}$ $vmhc^{+}$ cells suggests the possibility that midline signaling may play a role in ventricular specification, perhaps in conjunction with a more general influence on myocardial differentiation. Signals emanating from the prechordal plate may directly or indirectly produce differential responses within medial and lateral subsets of the precardiac mesoderm, creating the initial ventricular–atrial pattern (Fig. 8A).

Alternatively, cardiac chamber specification may occur much earlier, perhaps in conjunction with the initial induction of myocardial progenitors within the blastula. In this case, the medial location of ventricular precursors at the 15-somite stage would be merely a consequence of the cellular movements during and after gastrulation. At the initiation of gastrulation, the myocardial progenitors are thought to be clustered at the blastoderm margin bilaterally, near 90° and 270° longitude (Warga and Nüsslein-Volhard, 1999; Stainier *et al.*, 1993). Since fate maps of other mesodermal derivatives support conversion of a D–V orientation in the blastula to an A–P orientation within the organ (Kimmel *et al.*, 1990; Kozlowski *et al.*, 1997), we imagine that the cardiac chamber primordia could also be organized in a D–V orientation within the precardiac field (Figs. 8B and 8C). In this case, signals originating at the dorsal gastrula organizer could differentially influence dorsal and ventral portions of the precardiac field, thereby creating a precardiac pattern within the general mesodermal D–V pattern (Fig. 8B). Another influence could be the extraembryonic yolk syncytial layer (Fig. 8C), playing a role analogous to that of the extraembryonic endoderm during the early patterning of the murine A–P axis (Beddington and Robertson, 1998).

Further studies will be necessary to identify the specific tissues and molecules required for the initial specification of ventricular and atrial lineages as well as the precise role of *pan* in this process. The data presented here provide an important foundation for future analyses of the large collection of zebrafish mutations affecting cardiac A–P patterning and/or cardiac fusion (Alexander *et al.*, 1998; Chen *et al.*, 1996; Stainier *et al.*, 1996). These endeavors should lead to the assembly of genetic pathways that regulate the specification and differentiation of ventricular and atrial lineages, the choreography of cardiac fusion, and the coordination between these processes.

ACKNOWLEDGMENTS

We thank J. Alexander, D. Chu, E. Kupperman, C. Ott, A. Sehnert, and E. Walsh for comments on the manuscript and helpful discussions. We are also grateful to F. Stockdale and R. Breitbart for generous gifts of reagents and to A. Navarro for excellent fish care. The MF20 antibody was obtained from the Developmental Studies Hybridoma Bank, maintained by the Department of Biological Sciences, University of Iowa, under Contract NO1-HD-2-3144 from the NICHD. D.Y. is an Amgen fellow of the Life Sciences Research Foundation, and S.A.H. is a NSF predoctoral fellow. This work was supported by grants to D.Y.R.S. from the AHA, the Packard Foundation, and the March of Dimes.

REFERENCES

Alexander, J., Stainier, D. Y. R., and Yelon, D. (1998). Screening mosaic F1 females for mutations affecting zebrafish heart induction and patterning. *Dev. Genet.* **22,** 288–299.

Bader, D., Masaki, T., and Fischman, D. A. (1982). Immunochemical analysis of myosin heavy chain during avian myogenesis *in vivo* and *in vitro*. *J. Cell Biol.* **95,** 763–770.

Bao, Z. Z., Bruneau, B. G., Seidman, J. G., Seidman, C. E., and Cepko, C. L. (1999). Regulation of chamber-specific gene expression in the developing heart by Irx4. *Science* **283,** 1161–1164.

Beddington, R. S. P., and Robertson, E. J. (1998). Anterior patterning in mouse. *Trends Genet.* **14,** 277–284.

Chazaud, C., Chambon, P., and Dollé, P. (1999). Retinoic acid is required in the mouse embryo for left–right asymmetry determination and heart morphogenesis. *Development* **126,** 2589–2596.

Chen, J.-N., and Fishman, M. C. (1996). Zebrafish *tinman* homolog demarcates the heart field and initiates myocardial differentiation. *Development* **122,** 3809–3816.

Chen, J.-N., Haffter, P., Odenthal, J., Vogelsang, E., Brand, M., van Eeden, F. J., Furutani-Seiki, M., Granato, M., Hammerschmidt, M., Heisenberg, C. P., Jiang, Y.-J., Kane, D. A., Kelsh, R. N., Mullins, M. C., and Nüsslein-Volhard, C. (1996). Mutations affecting the cardiovascular system and other internal organs in zebrafish. *Development* **123,** 293–302.

Chen, J. N., DeSauvage, F., Hosobuchi, M., Jackson, D. G., and Fishman, M. C. (1998). Expressed sequences from the adult zebrafish heart. Unpublished results.

DeHaan, R. L. (1965). Morphogenesis of the vertebrate heart. In "Organogenesis" (R. L. DeHaan and H. Ursprung, Eds.), pp. 377–419. Holt, Rinehart and Winston, New York.

Fishman, M. C., and Chien, K. R. (1997). Fashioning the vertebrate heart: Earliest embryonic decisions. *Development* **124,** 2099–2117.

Franco, D., Lamers, W. H., and Moorman, A. F. (1998). Patterns of expression in the developing myocardium: Towards a morphologically integrated transcriptional model. *Cardiovasc. Res.* **38,** 25–53.

Garcia-Martinez, V., and Schoenwolf, G. C. (1993). Primitive-streak origin of the cardiovascular system in avian embryos. *Dev. Biol.* **159,** 706–719.

Goldstein, A. M., and Fishman, M. C. (1998). Notochord regulates cardiac lineage in zebrafish embryos. *Dev. Biol.* **201,** 247–252.

Kimmel, C. B., Warga, R. M., and Schilling, T. F. (1990). Origin and organization of the zebrafish fate map. *Development* **108,** 581–594.

Kozlowski, D. J., Murakami, T., Ho, R. K., and Weinberg, E. S. (1997). Regional cell movement and tissue patterning in the zebrafish embryo revealed by fate mapping with caged fluorescein. *Biochem. Cell Biol.* **75,** 551–562.

Lee, K. H., Xu, Q., and Breitbart, R. E. (1996). A new tinman-related gene, *nkx2.7,* anticipates the expression of *nkx2.5* and *nkx2.3* in zebrafish heart and pharyngeal endoderm. *Dev. Biol.* **180,** 722–731.

Lyons, G. E. (1994). In situ analysis of the cardiac muscle gene program during embryogenesis. *Trends Cardiovasc. Med.* **3,** 184–190.

Lyons, I., Parsons, L. M., Hartley, L., Li, R., Andrews, J. E., Robb, L., and Harvey, R. P. (1995). Myogenic and morphogenetic defects in the heart tubes of murine embryos lacking the homeobox gene *Nkx2-5. Genes Dev.* **9,** 1654–1666.

Moss, J. B., Xavier-Neto, J., Shapiro, M. D., Nayeem, S. M., McCaffery, P., Drager, U. C., and Rosenthal, N. (1998). Dynamic patterns of retinoic acid synthesis and response in the developing mammalian heart. *Dev. Biol.* **199,** 55–71.

Niederreither, K., Subbarayan, V., Dollé, P., and Chambon, P. (1999). Embryonic retinoic acid synthesis is essential for early mouse post-implantation development. *Nat. Genet.* **21,** 444–448.

O'Brien, T. X., Lee, K. J., and Chien, K. R. (1993). Positional specification of ventricular myosin light chain 2 expression in the primitive murine heart tube. *Proc. Natl. Acad. Sci. USA* **90,** 5157–5161.

Satin, J., Fujii, S., and DeHaan, R. L. (1988). Development of cardiac beat rate in early chick embryos is regulated by regional cues. *Dev. Biol.* **129,** 103–113.

Schulte-Merker, S., van Eeden, F. J., Halpern, M. E., Kimmel, C. B., and Nüsslein-Volhard, C. (1994). *no tail* (*ntl*) is the zebrafish homologue of the mouse *T* (*Brachyury*) gene. *Development* **120,** 1009–1015.

Searcy, R. D., and Yutzey, K. E. (1998). Analysis of Hox gene expression during early avian heart development. *Dev. Dyn.* **213,** 82–91.

Serbedzija, G. N., Chen, J. N., and Fishman, M. C. (1998). Regulation in the heart field of zebrafish. *Development* **125,** 1095–1101.

Stainier, D. Y. R., and Fishman, M. C. (1992). Patterning the zebrafish heart tube: Acquisition of anteroposterior polarity. *Dev. Biol.* **153,** 91–101.

Stainier, D. Y. R., Fouquet, B., Chen, J. N., Warren, K. S., Weinstein, B. M., Meiler, S. E., Mohideen, M. A., Neuhauss, S. C., Solnica-Krezel, L., Schier, A. F., Zwartkruis, F., Stemple, D. L., Malicki, J., Driever, W., and Fishman, M. C. (1996). Mutations affecting the formation and function of the cardiovascular system in the zebrafish embryo. *Development* **123,** 285–292.

Stainier, D. Y. R., and Gilbert, W. (1990). Pioneer neurons in the mouse trigeminal sensory system. *Proc. Nat. Acad. Sci. USA* **87,** 923–927.

Stainier, D. Y. R., Lee, R. K., and Fishman, M. C. (1993). Cardiovascular development in the zebrafish. I. Myocardial fate map and heart tube formation. *Development* **119,** 31–40.

Stalsberg, H., and DeHaan, R. L. (1969). The precardiac areas and formation of the tubular heart in the chick embryo. *Dev. Biol.* **19,** 128–159.

Warga, R. M., and Nüsslein-Volhard, C. (1999). Origin and development of the zebrafish endoderm. *Development* **126,** 827–838.

Westerfield, M. (1995). "The Zebrafish Book." Univ. of Oregon Press, Eugene, OR.

Xavier-Neto, J., Neville, C. M., Shapiro, M. D., Houghton, L., Wang, G. F., Nikovits, W. J., Stockdale, F. E., and Rosenthal, N. (1999). A retinoic acid-inducible transgenic marker of sino-atrial development in the mouse heart. *Development* **126,** 2677–2687.

Yutzey, K. E., and Bader, D. (1995). Diversification of cardiomyogenic cell lineages during early heart development. *Circ. Res.* **77,** 216–219.

Yutzey, K. E., Gannon, M., and Bader, D. (1995). Diversification of cardiomyogenic cell lineages *in vitro. Dev. Biol.* **170,** 531–541.

Yutzey, K. E., Rhee, J. T., and Bader, D. (1994). Expression of the atrial-specific myosin heavy chain AMHC1 and the establishment of anteroposterior polarity in the developing chicken heart. *Development* **120,** 871–883.

Received for publication May 28, 1999
Revised July 8, 1999
Accepted July 8, 1999